AIMS Materials Science, 6(5): 806–820.
DOI: 10.3934/matersci.2019.5.806
Received: 21 June 2019
Accepted: 30 August 2019
Published: 06 September 2019

http://www.aimspress.com/journal/Materials

Research article

Correlation of the chemical composition, structure and mechanical properties of basalt continuous fibers

Sergey I. Gutnikov*, Evgeniya S. Zhukovskaya, Sergey S. Popov and Bogdan I. Lazoryak

Chemistry Department, Lomonosov Moscow State University, Moscow 119991, Russia

* **Correspondence:** Email: gutnikov@gmail.com; Tel: +79266777505.

Abstract: This work presents the study of the dependence of the basalt continuous fibers (BCF) tensile strength on their chemical composition. 14 different basalt deposits were used to obtain continuous fibers by a laboratory scale system. Based on the data for more than 15 articles focused on natural basalt continuous fibers (32 different compositions) and experimental data of 14 experimental BCF series, the correlation of the tensile strength, the acid modulus and the *NBO/T* parameter was calculated. The PCC (pearson correlation coefficient) value of *NBO/T* and the tensile strength was 0.79, for acidity modulus and tensile strength −0.53.

Raman data for experimental BCF confirm the significant influence of the chemical composition of basalts on their structure, which determines their tensile strength. With a decrease in *NBO/T*, the observed ratio between the Raman bands at low- and high- frequencies gradually increases.

Keywords: basalt fiber; tensile strength; *NBO/T*; fiberglass structure

1. Introduction

Basalt continuous fibers (BCF) are a special kind of glass fibers which were first obtained in USSR in the 20th century. In distinction from widely used glass fibers (E-glass, AR-glass, S-glass, etc.), rocks are used as a raw material for the BCF production. Glasses based on basalts are multicomponent systems with the following composition (mass%): SiO_2 43–58, Al_2O_3 11–20,

CaO 7–13, FeO + Fe_2O_3 8–16, MgO 4–12, R_2O up to 4. Titanium dioxide often presents as well. However, the most basalt deposits have inconstant chemical composition [1]. Currently, BCF are perspective fillers for polymer composite materials and concretes because of their high mechanical properties [2,3] and alkali resistance [4–6].

BCF production technology is hampered due to the high crystallization ability of basalt melts and high fluctuations of the composition. As a result of these fundamental problems, the BCF production technology capacity is low and the BCF cost is high.

Several popular approaches are usually used to enhance mechanical properties of basalt continuous fibers. The first technique is thermal or chemical treatment [7–9]. The second technique is ion-exchange, which consists in displacing small alkali metal ions from the surface layer of heated glass by ions of large alkali metals [10]. An effective way to improve the mechanical properties of basalt fiber/epoxy resin composites is using special coating [11,12].

The study of the chemical composition influence on the mechanical and chemical properties of BCF usually comes down to the study of the effect of individual components of the composition [13,14]. According to some researchers, at least 46% silica (SiO_2) should be in BCF composition for a stable spinning process [15]. Higher percentage improves the spinning process and enhances the mechanical properties of fiber [16]. Most articles focus on the study of the effect of iron oxides [17,18]. The role of the ratio Fe^{3+}/Fe^{2+} is a subject of discussion [19,20], because the viscosity, density, mechanical properties, crystallization properties, and maximum service temperature have a strong dependence on iron redox amount [19–21]. It is believed that ferrous cations act as network modifiers with octahedral coordination while ferric ions are tetrahedrally coordinated network-former cations [22,23] when the ferric-ferrous ratio exceeds 1:2 [24].

To predict the mechanical properties, it is necessary to appreciate the reciprocal influence of different oxides in the basalt rock composition. Currently, the most commonly used parameter for that is acidity modulus (M_k). Usually, acidity modulus is calculated by the formula: $M_k = (Al_2O_3 + SiO_2)/(CaO + MgO)$, where Al_2O_3, SiO_2, CaO, MgO are oxides mass content [25–27]. In scientific articles, the composition of basalt fibers is also most often given in mass percentage [3,15,28].

To characterize the structure of aluminosilicate glasses, Mysen [29] proposed to consider the melt polymerization and the proportion of non-bridging oxygen atoms (NBO) to tetrahedral cations (T), known as the "*NBO/T*" parameter. There Si^{4+} and Al^{3+} are tetrahedrally coordinated network formers cations and Mg^{2+}, Ca^{2+}, and K^+, Na^+ ions are network modifiers that generate nonbridging oxygens. Mole fractions are used for calculation *NBO/T* [30]. This parameter is also calculated by a formula which takes into account the structural role of iron oxides [22,23]. It is extremely important for basalt systems.

In this work, it is proposed to use the *NBO/T* parameter to evaluate and predict the mechanical properties of basalt continuous fibers. BCF based on the 14 different basalt deposits were obtained and their mechanical properties were determined. Changes in the structure of basalt fibers were investigated by Raman spectroscopy.

2. Materials and methods

2.1. Preparation of glasses

Basalt rocks were ground and heated in a platinum crucible in a high temperature furnace at a rate of 250 °C/h up to 1000 °C and at 30 °C/h in the range of 1000–1600 °C, then homogenized at 1600 °C for 9 h. The molten glasses were quenched in water from 1600 °C.

2.2. X-ray fluorescence analysis

X-ray fluorescence analysis of the specimens was performed on a PAN Analytical Axios Advanced spectrometer. Characteristic X-rays were excited using a 4 kW Rh-anode X-ray tube. The excited radiation was recorded by a scanning channel with five exchangeable wave crystals and a detector. Measurements were made in transmission geometry in vacuum. Specimens were prepared in the form of pellets with a binder. The results are shown in Tables 1 and 2.

Table 1. The chemical composition (in mass%) of the continuous fibers based on 14 different basalt deposits.

Sample	SiO_2	Al_2O_3	TiO_2	FeO	Fe_2O_3	CaO	MgO	Na_2O
BCF 1	54.5	14.7	1.2	3.5	7.0	8.2	5.8	3.3
BCF 2	58.0	15.5	1.2	3.0	7.0	8.3	3.1	2.3
BCF 3	54.9	12.0	0.9	3.6	8.0	9.3	7.7	1.8
BCF 4	51.5	13.5	1.6	4.6	8.3	7.9	8.6	2.2
BCF 5	50.2	11.9	2.7	4.8	11.0	11.2	4.8	1.6
BCF 6	56.3	15.3	1.1	3.7	6.0	9.1	3.8	3.0
BCF 7	47.3	15.8	1.3	4.5	8.7	9.6	8.6	2.4
BCF 8	55.9	16.0	0.9	2.7	3.5	6.9	1.7	3.1
BCF 9	57.0	15.7	1.1	3.9	6.8	4.8	6.8	2.0
BCF 10	59.3	15.2	1.4	2.8	6.4	6.4	2.3	4.4
BCF 11	56.3	18.4	0.9	2.9	4.6	7.4	2.0	6.0
BCF 12	52.7	14.7	2.3	4.8	11.0	3.2	6.3	2.9
BCF 13	51.4	9.8	3.3	6.1	14.0	8.2	3.1	2.4
BCF 14	56.5	16.0	1.1	3.0	6.2	8.8	4.0	2.7

2.3. X-ray diffraction

X-ray diffraction (XRD) was made at room temperature on Thermo ARL X'TRA powder diffractometer ($CuK_{\alpha 1}$ radiation, λ = 1.54060 Å; $CuK_{\alpha 2}$ radiation, λ = 1.54443 Å). XRD patterns were collected in an angular range 2θ = 10–60° at a scan step 2θ = 0.02° and a scan rate of 1° (2θ)/min.

2.4. Production of fibers

Basalt continuous fibers were produced from prepared bulk glasses using a laboratory scale system [31]. Fiber formation was carried out under the temperature between 1400 and 1500 °C. Aminopropyltriethoxysilane sizing was applied in the fiber production.

2.5. Measuring of mechanical properties.

The tensile strength of the fibers was determined on a Hounsfield H100K-S universal tensile testing machine. Specimens were mounted in paper support frames using epoxy. The gauge length was 10 mm, and the crosshead speed was 5 mm/min (ISO 5079). The fibers had filament diameters of 10–12 μm. Measurement error of tensile strength is ±3%.

2.6. Raman spectroscopy

Raman spectra were collected on equipment, based on spectrometer TRIAX 552 (Jobin Yvon) and detector CCDSpec-10, 2KBUV (2048x512) (Princeton Instruments) in the range 200–2000 cm^{-1} with spectral resolution 1 cm^{-1}. The source of stimulating radiation was laser STABILITE 2017, laser stimulation of spectrum 514 nm. Fitting of the main envelopes and determination of band intensities were performed after long correction and baseline subtraction from raw data. For the treatment of data cubic baselines were used.

2.7. Calculation procedures

Acidity modulus is calculated by formula (Eq 1):

$$M_a = \frac{SiO_2 + Al_2O_3}{CaO + MgO} \quad (1)$$

where SiO_2, Al_2O_3, CaO, MgO are oxides mass fractions.

NBO/T is calculated according to [22,23], which are determined by Eq 2. The result is presented in the Table 3.

$$\frac{NBO}{T} = \frac{2\{[Na_2O] + [K_2O] + [CaO] + [MgO] + [MnO] - [FeO] - [Al_2O_3] - [Fe_2O_3]\}}{[SiO_2] + 2[Al_2O_3] + 2[Fe_2O_3] + [FeO] + [TiO_2] + [P_2O_5]} \quad (2)$$

In Eq 2 content of all oxides is given in mole fractions. Polymerization degree, that is defined as the number of non-bridging oxygen atoms per one formula unit number, has the maximum value at *NBO/T* = 0 (quartz SiO_2) and minimum at *NBO/T* = 4 (forsterite Mg_2SiO_4). If ratio Fe^{2+}/Fe^{3+} is not definitely determined it should be equal to 36:64 according to the Mössbauer spectroscopy data [20].

3. Results and discussion

3.1. Mechanical properties

At present, in the technical and regulatory documentation the acidity modulus is used for the description and selection of the raw materials for the basalt and glass fibers production. To calculate this parameter the formula, which includes the oxides mass content, is usually used [25–27].

In scientific articles, researchers also usually present composition data in mass percent. However, from a chemical point of view, the molar content of glass components is more significant.

For example, based on the molar concentration, the quantitative structural characteristic of glasses (*NBO/T*) is calculated. *NBO/T* is a ratio of nonbridging oxygens per tetrahedrally-coordinated cations. As shown, for example, by Mysen [29], this ratio represents polymerization degree of a silicate glass structure. For basalt glasses, a model was proposed that considered the high content of iron oxides. Based on the data from more than 15 articles concentrated on natural basalt continuous fibers (32 different compositions) (Tables 2 and 3), the correlation of the tensile strength of the filaments and the acid modulus and the *NBO/T* parameter was calculated. Using a simple linear approximation, it was found that the significance of the structural parameter is stronger. The PCClit (Pearson correlation coefficient) value of the *NBO/T* parameter was 0.69, and for *Ma* was 0.62 (Figure 1).

Table 2. The chemical composition (in mol%), acidity modulus (*Ma*), *NBO/T* and tensile strength of the continuous fibers based on 14 different basalt deposits (experimental) and literature data of natural basalt continuous fibers (32 different compositions).

Sample	SiO_2	Al_2O_3	TiO_2	FeO + Fe_2O_3	CaO	MgO	Na_2O	K_2O	Ref.
BCF 1	59.7	9.5	1.0	6.1	9.6	9.4	3.5	1.2	
BCF 2	64.5	10.1	1.0	5.6	9.8	5.2	2.5	1.2	
BCF 3	59.1	7.6	0.8	6.4	10.7	12.4	1.9	1.3	
BCF 4	55.9	8.6	1.3	7.6	9.2	13.9	2.3	1.2	
BCF 5	56.3	7.8	2.3	9.1	13.4	8.1	1.7	1.2	
BCF 6	62.0	9.9	0.9	5.9	10.7	6.3	3.2	1.2	
BCF 7	51.9	10.2	1.1	7.7	11.2	14.0	2.5	1.3	
BCF 8	66.9	11.3	0.8	4.3	8.9	3.1	3.6	1.2	
BCF 9	62.4	10.1	0.9	6.4	5.6	11.2	2.1	1.2	
BCF 10	66.1	10.0	1.2	5.3	7.7	3.9	4.7	1.2	
BCF 11	62.8	12.1	0.7	4.6	8.8	3.3	6.4	1.1	
BCF 12	59.9	9.8	2.0	9.2	3.9	10.6	3.2	1.3	
BCF 13	59.3	6.7	2.9	11.9	10.0	5.4	2.6	1.3	
BCF 14	62.3	10.4	0.9	5.4	10.4	6.5	2.9	1.2	
Myandukha	54.0	7.4	0.8	7.0	10.1	16.9	2.6	1.0	[32]
Kondopoga	57.6	8.9	1.2	6.0	7.6	10.7	5.0	2.6	
Berestovetskoe	55.2	8.3	2.4	8.4	11.5	9.2	3.3	1.4	
Marneul'skoe	55.5	10.8	1.5	6.0	10.6	7.6	5.2	2.7	
BF2	62.2	9.7	2.0	7.1	11.5	4.2	2.7	0.6	[28,33]
BF3	59.1	11.1	1.4	6.1	10.2	8.9	2.5	0.7	
BF4	59.3	9.6	1.2	7.0	8.9	9.0	4.5	0.5	
Sample 1	62	11.9	1.0	5.6	9.8	5.8	2.7	1.1	[34]
Sample 2	55.6	9.9	3.3	9.2	9.5	8.0	3.3	1.2	[35]
AN2	68.9	9.3	0.7	4.4	6.2	8.1	0.9	1.6	[36]
ANB1	61.5	9.2	1.1	7.6	8.0	8.5	3.6	0.5	
ANB2	62.3	9.5	0.8	6.0	7.4	8.4	3.6	2.1	
ANB3	62.6	12.2	1.0	6.2	6.3	6.1	4.4	1.2	
TB1	59.1	11.1	1.4	6.1	10.2	8.9	2.5	0.7	
TB2	58.9	10.4	1.8	6.8	7.7	9.6	3.6	1.3	
TB3	57.6	9.0	1.8	8.1	10.7	9.7	2.5	0.6	
TB4	56.6	11.7	2.4	6.9	9.6	8.9	3.1	0.8	
Sample 3	58	12.8	1.8	5.2	9.2	8.2	3	1.8	[37]
Sample 4	54.3	14.7	1.2	6.6	13.6	4.1	3.7	1.8	[13]
Sample 5	56.2	10.8	0.5	8.2	6.0	15.6	1.9	0.7	[38]
Sample 6	54.7	9.1	1.0	7.3	8.8	16.2	2.2	0.7	
Sample 7	57.5	9.8	0.7	5.9	12.3	10.8	2.3	0.7	
Sample 8	60.2	9.5	3.4	6.4	8.3	7.6	3.5	1.0	[39]
SB	47.5	11.4	2.1	6.9	10.6	15.7	4.0	1.7	[15]
CB1	62.7	10.2	1.0	6.6	9.0	6.8	2.6	1.1	
CB2	59.8	9.4	1.5	6.4	9.3	8.9	4.1	0.8	

Continued on next page

Sample	SiO_2	Al_2O_3	TiO_2	$FeO + Fe_2O_3$	CaO	MgO	Na_2O	K_2O	Ref.
CB3	57.2	12.0	0.9	6.6	10.7	8.7	2.6	1.2	[15]
Sample 9	61	10.6	1.3	7.1	8.9	6.8	3.6	0.7	[40]
Sample 10	59	11.7	0.0	5.9	10.7	7.6	4.4	0.5	[41]
Sample 11	62.7	10.2	1.0	6.6	9.0	6.8	2.6	1.1	[1]
B0	62.3	9.5	0.8	6.0	7.4	8.4	3.6	2.1	[14]
BCF	66.5	6.3	0.7	2.8	13.4	7.3	2.2	0.8	[42]

Table 3. The acidity modulus (*Ma*), *NBO/T and* tensile strength of the continuous fibers based on 14 different basalt deposits (experimental) and literature data of natural basalt continuous fibers (32 different compositions).

Sample	M_a	NBO/T	100 NBO/T	σ <MPa>	Ref.
BCF 1	5	0.209	20.9	2020	
BCF 2	6.5	0.080	8	2340	
BCF 3	3.9	0.288	28.8	2145	
BCF 4	3.9	0.244	24.4	2210	
BCF 5	3.9	0.168	16.8	2210	
BCF 6	5.5	0.121	12.1	2860	
BCF 7	3.5	0.263	26.3	1495	
BCF 8	8.3	0.025	2.5	2574	
BCF 9	6.2	0.078	7.8	2730	
BCF 10	8.5	0.046	4.6	2834	
BCF 11	8	0.063	6.2	2470	
BCF 12	7.1	0.000	0.0	3380	
BCF 13	5.4	0.017	1.7	3211	
BCF 14	5.7	0.115	11.5	3133	
Myandukha	3.2	0.374	37.4	1200	[32]
Kondopoga	5.1	0.277	27.7	1200	
Berestovetskoe	4.1	0.237	23.7	1200	
Marneul'skoe	4.9	0.250	25.0	1200	
BF2	5.8	0.066	6.6	2452	[28,33]
BF3	5.0	0.145	14.5	2949	
BF4	5.3	0.174	17.4	2965	
Sample 1	6.3	0.058	5.8	2728	[34]
Sample 2	5.1	0.088	8.8	2600	[35]
AN2	7.5	0.082	8.2	2175	[36]
ANB1	5.8	0.108	10.8	3370	
ANB2	6.3	0.159	15.9	3063	
ANB3	8.3	−0.011	−1.1	3075	
TB1	5.0	0.145	14.5	2949	
TB2	5.6	0.145	14.5	2936	
TB3	4.4	0.176	17.6	2452	
TB4	5.1	0.114	11.4	2253	
Sample 3	5.7	0.123	12.3	2850	[37]
Sample 4	5.1	0.067	6.8	2300	[13]
Sample 5	4.6	0.158	15.8	1800	[38]
Sample 6	3.7	0.292	29.2	1900	
Sample 7	4	0.263	26.3	1900	
Sample 8	5.9	0.125	12.5	2600	[39]
SB	3.3	0.355	35.4	602	[15]
CB1	6.2	0.078	7.8	2016	
CB2	5.2	0.194	19.4	1608	
CB3	4.9	0.140	14.0	1811	
Sample 9	6.1	0.069	6.9	2490	[40]
Sample 10	5.2	0.160	16.0	2457	[41]
Sample 11	6.2	0.078	7.8	2307	[1]
B0	6.3	0.160	15.9	3153	[14]
BCF	4.4	0.305	30.5	1702	[42]

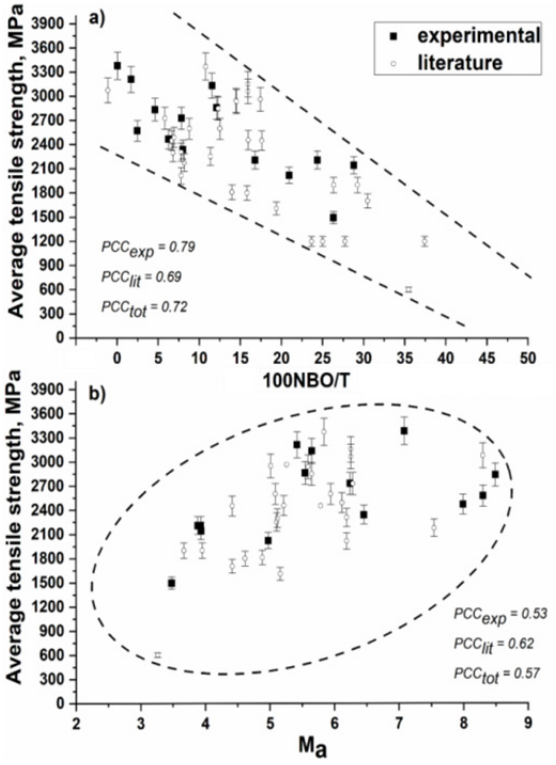

Figure 1. Experimental data for continuous fibers based on basalt from 14 different deposits and literature data for 15 basalt fibers with different compositions. (a) The dependence of the tensile strength of the filaments on the *NBO/T* parameter. (b) The dependence of the tensile strength of the filaments on the acid modulus. PCC_{exp}—Pearson correlation coefficient of the experimental data, PCC_{lit}—Pearson correlation coefficient of the literature data, PCC_{tot}—Pearson correlation coefficient of the literature and experimental data.

Thus, we concluded that *NBO/T* can be used as the parameter to estimate the BCF mechanical properties. The calculated Pearson correlation coefficients are close to each other. In our opinion, this is due to many different factors that can affect the value of BCF tensile strength. These factors do not coincide in different sources and often are not specified. Not only the chemical composition but also other factors could affect the BCF tensile strength: the laboratory plant scheme, the tensile strength measuring method, the fiber diameter, the melt temperature and others.

To confirm the proposed approach, a series of BCF samples based on 14 different basalt deposits were obtained under equal conditions. Basalt continuous fibers were produced using a laboratory scale system [42]. According to X-ray diffraction, all obtained samples are amorphous. The basalt filaments chemical composition in mass% is given in Table 1. To minimize the impact of different factors on the tensile strength, the following conditions were chosen: the same fiber diameter (about 10–12 μm), the same tensile strength measuring method (according to ISO 5079), the same melt temperature (about 1600 °C).

The tensile strength of the experimental BCF varies in the range from 1495 to 3380 MPa. Literature data spread is wider (from 602 to 3370 MPa) [15,36]. This is due to the fact that the fibers

are obtained in different conditions. Moreover, the chemical composition of the fibers affects not only their structure, but also the production conditions. In [36], 8 samples of basalt fibers of various compositions were studied. The chemical composition varies within the following limits (mol%): SiO_2 56.6–68.9, Al_2O_3 9–12.2, CaO 6.2–10.7, FeO + Fe_2O_3 4.4–8.1, MgO 6.1–9.7, Na_2O 0.9–4.4, K_2O 0.9–4.4, TiO_2 0.7–2.4. For experimental samples, SiO_2 51.9–66.9, Al_2O_3 6.7–12.1, CaO 3.9–13.4, FeO + Fe_2O_3 4.3–11.9, MgO 3.1–14, Na_2O 1.7–6.4, K_2O 1.1–1.3, TiO_2 0.7–2.9. The tensile strength of the experimental samples and samples obtained in [36] is also close. The worst fiber tensile strength in series was 2253 MPa. The average value of the tensile strength of the BCF series was about 2900 MPa, and the highest filament tensile strength was 3370 MPa. For experimental samples the worst fiber tensile strength was 1495 MPa and the highest filament tensile strength was 3380 MPa.

The dependence of the obtained filaments tensile strength on the *NBO/T* parameter and acid modulus was calculated. The PCCexp (Pearson correlation coefficient) value for the *NBO/T* parameter was 0.79, and for *Ma* −0.53. Based on experimental data, it can be concluded that for the samples obtained under identical conditions, the correlation between the structural parameter and the tensile strength is much higher than the correlation between the acidity modulus and the tensile strength.

Tables 2 and 3 shows the experimental data for continuous fibers based on 14 different basalt deposits and literature data for 15 basalt fibers with different compositions. The PCCtot value of the *NBO/T* and tensile strength was 0.73, for *Ma* −0.60. We would like to note that in the scientific articles the chemical composition of all BCF was presented in mass percent (Figure 1).

The correlation between the chemical composition and tensile strength of a glass continuous fiber has been studied for a long time. According to many authors, the increase in the content of glass-forming oxides (aluminum or silicon oxides) should lead to increased strength [14]. In this case, the quartz fibers should have maximum strength. In practice, this is not true. The maximum strength for glass fibers is observed for S-glass fibers. This fact is due to the strength of glass network of aluminosilicate glass fibers, is governed by local atom coordination. There is no universal law for the effect of composition on tensile strength because the glass structure changes with composition as does the valence of certain oxides.

The absence of a long-range order in the structure of glass leads to the fact that the strength of fibers is determined not only by their chemical composition, but also by the valence of cations. This is especially important for basalt fibers, since they contain a large amount of iron oxides. The presence of higher field strengths ions, such as Mg^{2+} or Zn^{2+} [10], leads to strengthening of the glasses. At the same time, the effective increase of glass strength can be achieved by increasing the relative amount of network formers, such as AlIV [13]. Aluminum cations can be found both in tetrahedral and octahedral coordination in the structure of aluminosilicate glasses. Aluminum in fourfold coordination (AlIV) is a network former but AlVI is a network modifier. The ratio of the number of cations with different coordination depends on the chemical composition of the glass [42].

Table 4 shows the Pearson correlation coefficient of the tensile strength and the oxide content (molar and mass) for the experimental data of the BCF based on 14 different basalt deposits, the literature data of 15 basalt continuous fibers with different compositions and the both series.

The strong dependence is observed for the molar content of silicon oxide, alkali metal oxides (R_2O) and alkaline earth metal oxides (RO). Both for experimental and literature data the PCC of the SiO_2 molar content and the tensile strength was about 0.5. The PCC is lower for the same oxide content expressed in mass fractions. That confirms our approach. The influence of the SiO_2 content on BCF mechanical properties is noted by many researchers. As shown in article [36], BCF tensile strength decreases with decreasing silicon oxide content, which is explained by the fact that SiO_2 can strengthen basalt glass network structures, as well as form network structures and increase the tensile strength of basalt fibers. The same effect could be expected for Al_2O_3. However, strong correlation in this case is possible only in a definite composition interval, since aluminum atoms can act both as network former and as modifiers [13].

The content of alkaline-earth RO cations has a significant effect. Calculated PCC of the tensile strength and RO content are high for both literature and experimental data. An increase in the content of CaO and MgO oxides in basalts may lead to an increase in the ability to basalt fibers crystallization on their base [32]. That leads to a significant reduction in the BCF tensile strength. High concentration in the composition of the modifiers (Na_2O, K_2O, CaO, MgO) leads to reduce the tensile strength of the fibers [10]. Our calculations also confirm the effect of alkaline cations on tensile strength (Table 4).

Table 4. The PCC values of the tensile strength and the oxide content (molar and mass) for the experimental data of BCF based on 14 different basalt deposits (PCC (experimental)), literature data for 15 basalt continuous fibers with different compositions (PCC (literature)) and both series (PCC (total)). R_2O—alkali metal oxides ($Na_2O + K_2O$), RO—alkaline earth metal oxides (MgO + CaO).

Content	PCC	SiO_2	Al_2O_3	TiO_2	$FeO + Fe_2O_3$	CaO	MgO	Na_2O	K_2O	R_2O	RO
Molar	Experimental	0.52	0.01	0.34	0.25	0.45	0.18	0.03	0.53	0.54	0.46
	Literature	0.50	0.24	0.02	0.24	0.49	0.04	0.26	0.62	0.39	0.50
	Total	0.52	0.14	0.05	0.12	0.48	0.01	0.22	0.57	0.45	0.50
Mass	Experimental	0.40	0.08	0.33	0.15	0.55	0.46	0.15	0.21	0.14	0.69
	Literature	0.29	0.18	0.05	0.39	0.38	0.51	0.08	0.30	0.22	0.66
	Total	0.35	0.08	0.02	0.22	0.41	0.49	0.02	0.26	0.15	0.65

In our opinion, the *NBO/T* parameter is a complex character of the glass structure with the definite composition. *NBO/T* better considers the correlation of the chemical composition and the BCF tensile strength for multicomponent systems. A comparison of the literature data and the obtained experimental data shows that the production of fibers with high strength (above 2800 MPa) is customary to the following composition range mol%: SiO_2 58–66.1, Al_2O_3 6.7–12.8, CaO 3.9–10.7, $FeO + Fe_2O_3$ 5.2–11.9, MgO 3.9–10.6, Na_2O 2.5–4.7, K_2O 0.5–2.1, TiO_2 0.8–2.9. The results are consistent with each other and can be the basis for creating regulatory documentation similar to ASTM D578.

3.2. Raman spectra

One of the widely used method of investigating the structure of glasses is the Raman spectroscopy. The Raman spectra of all basalt continuous fibers obtained based on 14 different deposits are presented in Figure 2. The Raman spectra of all analyzed basalt fibers are characterized by three regions: low-frequency region (LF: ~200–600 cm^{-1}), middle-frequency region (MF: ~600–800 cm^{-1}) and high-frequency region (HF: ~800–1200 cm^{-1}). The intensity observed in the spectra increases from high wave numbers to low ones. Similar areas can be observed in synthetic natural glass [21,43].

The LF-envelope can be explained as a convolution of delocalized vibration modes, associated mainly with symmetric stretching of bridging oxygen bonds, bending vibration of silicon polyhedra, the rings breathing modes [44]. The intensity of HF-envelope shows the relative concentrations of silica tetrahedra with one (1100 cm^{-1}), two (about 1000–950 cm^{-1}) and four (about 800–850 cm^{-1}) non-bridging oxygen atoms [45]. The high-frequency region falls into the stretching vibrations of disilicate, metasilicate, pyrosilicate and orthosilicate. This region reflects the modification of inter-tetrahedral bond angles, force constants, T–O distances and polymerization due to the action of network modifying and charge balancing cations [21].

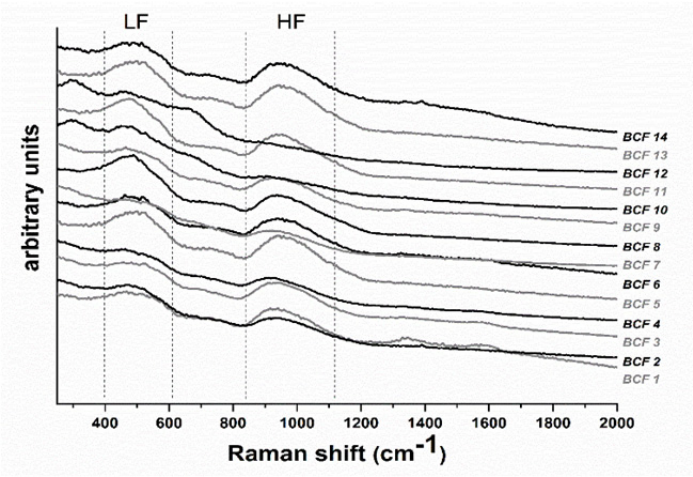

Figure 2. Raman spectra of the continuous fibers based on basalt from 14 different deposits. LF is low-frequency region and HF is high-frequency region.

The methodology of spectrum analysis differs slightly from one researcher to another. It depends on the composition of the glass. For quantitative analysis of basalt and other natural glasses Raman spectra, it is usually applied recalculation of the raw spectra (I(ν)) to a format (R(ν)) as proposed by Long [43]. Therefore, curves fitting and calculation of band intensities of Raman data for all obtained basalt fibers were performed after Long correction and cubic baseline subtraction (Figure 3).

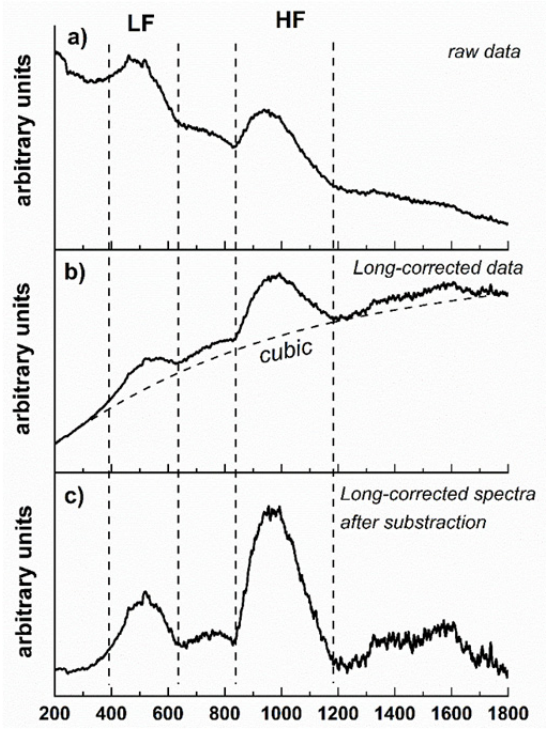

Figure 3. Example of long correction and baseline subtraction of Raman spectra: (a) raw data of Raman spectra, (b) long-corrected Raman spectra, and (c) subtracted long-corrected Raman spectra.

It is known that the degree of polymerization of aluminosilicate glasses affects the intensity of the bands in the Raman spectra, hence, the amount of non-bridge oxygens (O^-) also influences. With a decrease in *NBO/T*, the observed ratio between intensity of the two main Raman spectra regions at low and high frequencies gradually increases in both synthetic and natural glasses [45,46]. The authors showed that the I_{LF}/I_{HF} ratio (I_{LF}—low-frequency region intensity, I_{HF}—high-frequency region intensity) exponentially decreases from 3 to 2 in low *NBO/T* rhyolitic glasses and down to 0.6–0.3 in high NBO/T mafic basanites and tephrites. The rate of decline is very sharp in in the *NBO/T* range 0–0.1, while the I_{LF}/I_{HF} ratio is near invariable in glasses with high *NBO/T* amount [47]. Figure 4 shows the correlation of the I_{LF}/I_{HF} ratio and *NBO/T* of continuous fibers obtained on the basis of 14 different deposits. I_{LF}/I_{HF} ratio exponentially decreases from 2.6 to 1 in low *NBO/T* basalt fibers and down to 0.8–0.3 in high *NBO/T* (Figure 4).

The chemical composition of basalt glasses and fibers on their base directly determines the intensity of peaks in low and high regions of Raman spectra. The increase in the composition of alkaline earth ions and alkali ions leads to depolymerization of the glass structure with the formation of the NBO, which leads to a decrease I_{LF}/I_{HF}. The increasing the modifiers content in basalt composition causes a shift of high-frequency band positions toward lower wave numbers in Si–O–Si stretching band. The fact that the main Si–O–Si absorption band begins to shift to lower wave number is interpreted to mean that some of the aluminum ions are in different local surroundings [10]. With the addition of alkali oxides, the nonbridging oxygen ions are converted to bridging oxygen ions, as the aluminum ions must use some of the nonbridging oxygen ions to form

AlO_4 tetrahedra. In glasses with high contents of alkali oxides, the aluminum is mostly in the fourfold coordination (AlO_4 tetrahedra) that forms together with the SiO_4 tetrahedra the aluminosilicate glass network [13]. The presence of aluminum helps the glass to retain regions with a highly polymerized structure At the same time, it should be taken into account that at their high content, glass can be stratified, which leads to the formation of the regions with a high content of silicon oxide, different from that which can be expected theoretically. For basalt fibers Raman bands related to Q4 species and Fe^{3+} band directly correlate with the changes in degree of polymerization of the structure [21,44].The results of the dependence of *NBO/T* and the ratio I_{LF}/I_{HF} of the Raman spectra for basalt fiber samples obtained from 14 basalt deposits are confirm the significant influence of the chemical composition of basalts on their structure, which determines their tensile strength (Figure 4). The use of *NBO/T* will allow to predict the properties of basalt continuous fibers more accurately when choosing a deposit for their production.

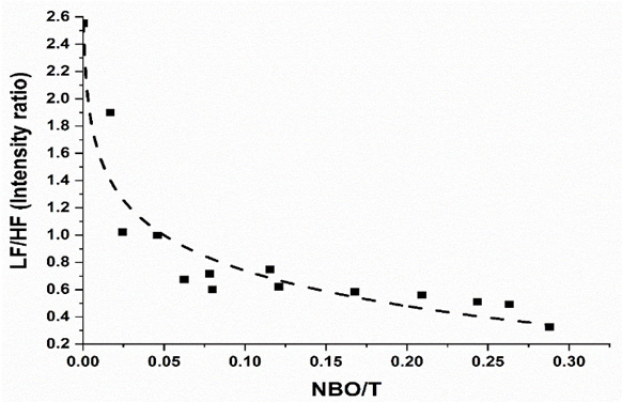

Figure 4. The correlation between the I_{LF}/I_{HF} ratio and *NBO/T* of continuous fibers obtained based on 14 different basalt deposits.

4. Conclusion

The series of BCF samples based on 14 different basalt deposits was obtained under equal conditions. The tensile strength of the fibers from different deposits varies in the range from 1495 to 3380 MPa. Based on the literature data, the dependence of the tensile strength of the filaments on the acid modulus and the *NBO/T* parameter about 32 natural basalt continuous fibers with different compositions and experimental data about 14 obtained BCF series was calculated. The PCC (Pearson correlation coefficient) value of the *NBO/T* and the tensile strength was 0.79, for acidity modulus and tensile strength −0.53. Thus, the correlation between the structural parameter and strength is higher than the correlation between the acidity and strength modulus.

Basalt continuous fibers obtained on the basis of 14 different deposits were investigated by Raman spectroscopy. Using long correction, the correlation between the I_{LF}/I_{HF} ratio and *NBO/T* of continuous fibers obtained on the basis of 14 different deposits was determined. I_{LF}/I_{HF} ratio exponentially decreases from 2.6 to 1 in low *NBO/T* basalt fibers and down to 0.8–0.3 in high *NBO/T*.

Acknowledgements

This work was supported by Russian Foundation for Basic Research (grant no. 18-38-00483).

Conflict of interests

The authors declare no conflicts of interests.

References

1. Sarasini F, Tirillò J, Seghini MC (2018) Influence of thermal conditioning on tensile behaviour of single basalt fibres. *Compos Part B-Eng* 132: 77–86.
2. Fiore V, Scalici T, Di Bella G, et al. (2015) A review on basalt fibre and its composites. *Compos Part B-Eng* 74: 74–94.
3. Wei B, Cao H, Song S (2010) Tensile behavior contrast of basalt and glass fibers after chemical treatment. *Mater Design* 31: 4244–4250.
4. Overkamp T, Mahltig B, Kyosev Y (2018) Strength of basalt fibers influenced by thermal and chemical treatments. *J Ind Text* 47: 815–833.
5. Lee JJ, Song J, Kim H (2014) Chemical stability of basalt fiber in alkaline solution. *Fiber Polym* 15: 2329–2334.
6. Scheffler C, Förster T, Mäder E, et al. (2009) Aging of alkali-resistant glass and basalt fibers in alkaline solutions: evaluation of the failure stress by Weibull distribution function. *J-Non Cryst Solids* 355: 2588–2595.
7. Lezzi PJ, Xiao QR, Tomozawa M, et al. (2013) Strength increase of silica glass fibers by surface stress relaxation: A new mechanical strengthening method. *J-Non Cryst Solids* 379: 95–106.
8. Jain N, Singh VK, Chauhan S (2017) Review on effect of chemical, thermal, additive treatment on mechanical properties of basalt fiber and their composites. *J Mech Behav Mater* 26: 205–211.
9. Sabet SMM, Akhlaghi F, Eslami-Farsani R (2015) The effect of thermal treatment on tensile properties of basalt fibers. *J Ceram Sci Tech* 6: 245–248.
10. Kuzmin KL, Zhukovskaya ES, Gutnikov SI, et al. (2016) Effects of ion exchange on the mechanical properties of basaltic glass fibers. *Int J Appl Glass Sci* 7: 118–127.
11. Li Z, Xiao T, Zhao S (2016) Effects of surface treatments on Mechanical properties of Continuous basalt fibre cords and their Adhesion with rubber matrix. *Fiber Polym* 17: 910–916.
12. Gauvin F, Cousin P, Robert M (2015) Improvement of the interphase between basalt fibers and vinylester by nano-reinforced post-sizing. *Fiber Polym* 16: 434–442.
13. Gutnikov SI, Malakho AP, Lazoryak BI, et al. (2009) Influence of alumina on the properties of continuous basalt fibers. *Russ J Inorg Chem* 54: 191–196.
14. Liu J, Yang J, Chen M, et al. (2018) Effect of SiO_2, Al_2O_3 on heat resistance of basalt fiber. *Thermochim Acta* 660: 56–60.

15. Deák T, Czigány T (2009) Chemical composition and mechanical properties of basalt and glass fibers: A comparison. *Text Res J* 79: 645–651.
16. Bauer F, Kempf M, Weiland F, et al. (2018) Structure-property relationships of basalt fibers for high performance applications. *Compos Part B-Eng* 145: 121–128.
17. Karamanov A, Pisciella P, Cantalini C, et al. (2000) Influence of Fe^{3+}/Fe^{2+} ratio on the crystallization of iron-rich glasses made with industrial wastes. *J Am Ceram Soc* 83: 3153–3157.
18. Karamanov A, Pelino M (2001) Crystallization phenomena in iron-rich glasses. *J Non-Cryst Solids* 83: 139–151.
19. Moiseev EA, Gutnikov SI, Malakho AP, et al. (2008) Effect of iron oxides on the fabrication and properties of continuous glass fibers. *Inorg Mater* 44: 1026–1030.
20. Manylov MS, Gutnikov SI, Lipatov YV, et al. (2015) Effect of deferrization on continuous basalt fiber properties. *Mendeleev Commun* 5: 386−388.
21. Di Genova D, Vasseur J, Hess KU, et al. (2017) Effect of oxygen fugacity on the glass transition, viscosity and structure of silica- and iron-rich magmatic melts. *J-Non Cryst Solids* 470: 78–85.
22. Brooker RA, Kohn SC, Holloway JR, et al. (2001) Structural controls on the solubility of CO_2 in silicate melts Part I : bulk solubility data. *Chem Geol* 174: 225–239.
23. Persikov ES, Bukhtiyarov PG, Sokol AG (2017) Viscosity of hydrous kimberlite and basaltic melts at high pressures. *Russ Geol Geophys* 58: 1093–1100.
24. Smith DR, Cooper RF (2000) Dynamic oxidation of a Fe^{2+}-bearing calcium–magnesium–aluminosilicate glass: the effect of molecular structure on chemical diffusion and reaction morphology. *J-Non Cryst Solids* 278: 145–163.
25. Ma Z, Tian X, Liao H, et al. (2018) Improvement of fly ash fusion characteristics by adding metallurgical slag at high temperature for production of continuous fiber. *J Clean Prod* 171: 464–481.
26. Perevozchikova BV, Pisciotta A, Osovetsky BM, et al. (2014) Quality evaluation of the Kuluevskaya basalt outcrop for the production of mineral fiber, Southern Urals, Russia. *Energ Procedia* 59: 309–314.
27. Vasil'eva AA, Kychkin AK, Anan'eva ES, et al. (2014) Investigation into the properties of basalt of the Vasil'evskoe deposit in Yakutia as the raw material for obtaining continuous fibers. *Theor Found Chem En* 48: 667–670.
28. Chen X, Zhang Y, Huo H, et al. (2017) Improving the tensile strength of continuous basalt fiber by mixing basalts. *Fiber Polym* 18: 1796–1803.
29. Mysen BO, Virgo D, Scarfe CM (1980) Relations between the anionic structure and viscosity of silicate melts—a Raman spectroscopic study. *Am Mineral* 65: 690–710.
30. Mysen BO, Virgo D, Seifert FA (1982) The structure of silicate melts: implications for chemical and physical properties of natural magma. *Rev Geophys* 20: 353–383.
31. Gutnikov SI, Manylov MS, Lipatov YV, et al. (2013) Effect of the reduction treatment on the basalt continuous fiber crystallization properties. *J-Non Cryst Solids* 368: 45–50.
32. Morozov NN, Bakunov VS, Morozov EN, et al. (2001) Materials based on basalts from the european north of Russia. *Glass Ceram* 58: 100–104.

33. Chen X, Zhang Y, Hui D, et al. (2017) Study of melting properties of basalt based on their mineral components. *Compos Part B-Eng* 116: 53–60.
34. Shebanov SM, Novikov IK, Koudryavtsev AA, et al. (2018) Strength characteristics of the filaments and a basalt fiber roving at different clamping lengths and deformation rates. *Mech Compos Mater* 54: 349–350.
35. Wei B, Cao H, Song S (2010) Tensile behavior contrast of basalt and glass fibers after chemical treatment. *Mater Design* 31: 4244–4250.
36. Chen X, Zhang Y, Huo H, et al. (2018) Study of high tensile strength of natural continuous basalt fibers. *J Nat Fibers* 1–9.
37. Kessler E, Gadow R, Straub J (2016) Basalt, glass and carbon fibers and their fiber reinforced polymer composites under thermal and mechanical load. *AIMS Mater Sci* 3: 1561–1576.
38. Dzhigiris DD, Makhova MF, Gorobinskaya VD, et al. (1983) Continuous basalt fiber. *Glass Ceram* 40: 467–470.
39. Wei B, Cao H, Song S (2010) Environmental resistance and mechanical performance of basalt and glass fibers. *Mater Sci Eng A-Struct* 527: 4708–4715.
40. Bhat T, Fortomaris D, Kandare E, et al. (2018) Properties of thermally recycled basalt fibres and basalt fibre composites. *J Mater Sci* 53: 1933–1944.
41. Chen Z, Huang Y (2016) Mechanical and interfacial properties of bare basalt fiber. *J Adhes Sci Technol* 30: 2175–2187.
42. Kuzmin KL, Gutnikov SI, Zhukovskaya ES, et al. (2017) Basaltic glass fibers with advanced mechanical properties. *J-Non Cryst Solids* 476: 144–150.
43. Di Genova D, Morgavi D, Hess KU, et al. (2015) Approximate chemical analysis of volcanic glasses using Raman spectroscopy. *J Raman Spectrosc* 46: 1235–1244.
44. Welsch AM, Knipping JL, Behrens H (2017) Fe-oxidation state in alkali-trisilicate glasses—A Raman spectroscopic study. *J-Non Cryst Solids* 471: 28–38.
45. White WB, Minser DG (1984) Raman spectra and structure of natural glasses. *J-Non Cryst Solids* 67: 45–59.
46. Di Muro A, Métrich N, Mercier M, et al. (2009) Micro-Raman determination of iron redox state in dry natural glasses: application to peralkaline rhyolites and basalts. *Chem Geol* 259: 78–88.
47. Mercier M, Di Muro A, Giordano D, et al. (2009) Influence of glass polymerisation and oxidation on micro-Raman water analysis in alumino–silicate glasses. *Geochim Cosmochim Ac* 73: 197–217.